

Supporting Information

Achieving Efficient Near-Ultraviolet HLCT Emitters based on Isomer Engineering

Shuyuan Ge,^a Yixuan Jiang,^a Zhuang Cheng,^a Yi Sak Lee,^b Xiaoen Shi,^a Yifu Zhao,^a Taekyung Kim,^{*c} and Ping Lu^{*a}

^a State Key Laboratory of Supramolecular Structure and Materials, College of Chemistry, Jilin University, 2699 Qianjin Avenue, Changchun 130012, China

^b Department of Information Display, Hongik University, Seoul 04066, Korea

^c Department of Chemical Engineering, Kyung Hee University, Yongin-si, Gyeonggi-do, 17104, Korea

*Corresponding author: lup@jlu.edu.cn; taekyung.kim@khu.ac.kr

Contents

1. General Information	S2
2. Synthesis and Characterization	S3
3. Thermal Properties	S11
4. Theoretical Calculations	S12
5. Cyclic Voltammetry Measurement	S14
6. Photophysical Properties	S14
7. Electroluminescence	S16
References	S16

1. General Information

¹H and ¹³C NMR spectra were measured on a spectrometer with model of Bruker AVANCE 500, tetramethylsilane were used as the internal standard. The final compounds were characterized by the MALDI-TOF mass spectra based on an AXIMA-CFR™ plus instrument. On a Flash EA 1112, CHNS-O elemental analysis instrument, elemental analysis was performed. Thermal gravimetric analysis was tested based on a thermal analysis system of Perkin-Elmer and measured from 50 °C to 800 °C with a heating rate of 10 °C min⁻¹. A NETZSCH unit with DSC-204 model was used to record differential scanning calorimetry measured from 30 °C to 380 °C upon a heating rate of 10 °C min⁻¹. The electrochemical properties were performed via cyclic voltammetry (CV) measurements. The tests used a standard one-compartment, three-electrode electrochemical cell given by a BAS 100B W⁻¹ electrochemical analyzer, where tetrabutylammoniumhexafluorophosphate (TBAPF₆) in anhydrous dimethyl formamide (DMF) or anhydrous dichloromethane (DCM) with the concentration of 0.1 M were used as the electrolytes for negative or positive scans to calculate the oxidation and reduction potentials of the materials. The resulting HOMO/LUMO values are calculated according to the equation: (unit: eV)

$$E_{\text{HOMO}} = -(E_{\text{ox}} \text{ vs. Fc/Fc}^+ + 4.8) \quad \text{Equation S1}$$

$$E_{\text{LUMO}} = -(E_{\text{red}} \text{ vs. Fc/Fc}^+ + 4.8) \quad \text{Equation S2}$$

UV-vis spectra of solutions were measured on a UV-3100 Spectrophotometer made by Shimadzu. Steady-state photoluminescence spectra and lifetimes were carried out with FLS980 Spectrometer. Quantum efficiencies in film and crystal were measured using an integrating sphere apparatus. The phosphorescence spectra were measured at 77 K in tetrahydrofuran based on an Edinburgh spectrometer LP920.

The k_r and k_{nr} mentioned are calculated according to the equations:

$$k_r = \frac{\varphi}{\tau} \quad \text{Equation S3}$$

$$k_{\text{nr}} = \frac{1 - \varphi}{\tau} \quad \text{Equation S4}$$

where φ is the PLQY measured by an integrating sphere attachment of FLS920 spectrophotometer, τ is the corresponding lifetimes of the emitters.

Device fabrication: the substrate was ITO coated glass with the sheet resistance of 20 Ω square⁻¹. Toluene, acetone, isopropyl alcohol and deionized water were used to clean the ITO

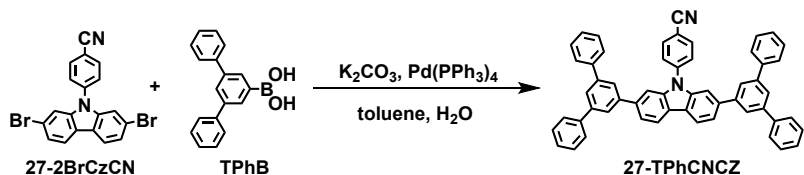
glass substrates under ultrasonic condition, then dried at 120 °C in an air oven. Afterwards the substrates were treated with UV-zone for 30 min, and prepared in a vacuum deposition system for organic and metal deposition under a base pressure of less than 5×10^{-6} mbar. All organic layers were deposited at a rate of 1.0 Å s⁻¹. Deposition rates of 0.1 Å s⁻¹ and 4.0 Å s⁻¹ were adjusted for the cathode LiF (1 nm) and then the capping Al metal layer (100 nm), respectively. The electroluminescent properties were evaluated base on a programmable electrometer with model of Keithley 2400 and a Spectroscan spectrometer with model of PR-650 at room temperature.

Density functional theory (DFT) was carried out for the ground-state geometry optimization at the level of PBE0/6-31G(d,p) using Gaussian 09 (version A.03) package on a Power Leader cluster. Time-dependent density functional theory (TD-DFT) was carried out for natural transition orbitals (NTOs) at the level of PBE0/6-31G(d,p).

2. Synthesis and Characterization

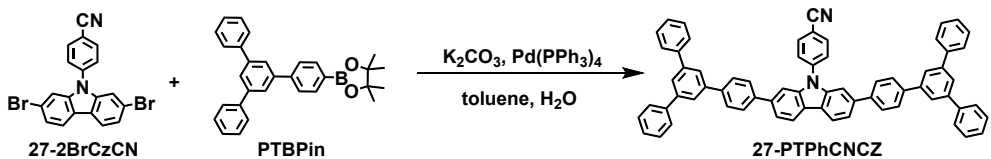
The intermediates 27-2BrCzCN and 36-2BrCzCN were synthesized following a literature procedure [1]. All starting materials and solvents were obtained from Energy Chemical and Bide Pharmatech Ltd. All final products were purified prior to characterization.

27-TPhCNCZ:



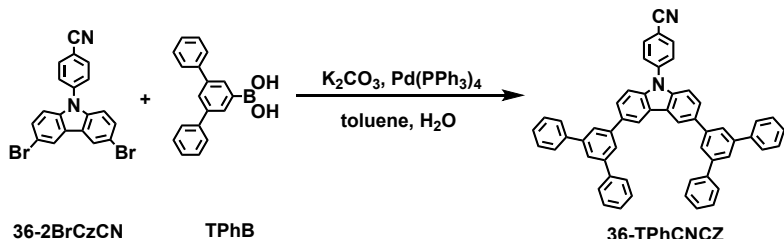
In a 100 mL round flask, a mixture of 27-2BrCzCN (0.46 g, 1 mmol), TPhB (0.66 g, 2.4 mmol), K₂CO₃ (5.52 g, 40 mmol), distilled water (20 mL), toluene (40 mL) and Pd(PPh₃)₄ (0.03 g, 0.03 mmol) was added and refluxed at 90 °C under N₂ atmosphere for 24 hours. The reaction was then quenched by water and the mixture was extracted with dichloromethane for three times. After evaporation of the solvent, the residue was purified via column chromatography and got white solid. (Yield: 63%). ¹H NMR (500 MHz, CD₂Cl₂) δ (ppm): 8.34 (d, J = 6.4 Hz, 2H), 7.99 (d, J = 6.8 Hz, 2H), 7.90 (d, J = 1.2 Hz, 5H), 7.87 (d, J = 4.7 Hz, 3H), 7.82 – 7.72 (m, 12H), 7.54 (t, J = 6.1 Hz, 8H), 7.45 (t, J = 5.9 Hz, 4H). ¹³C NMR (151 MHz, CD₂Cl₂) δ 142.79, 142.41, 141.63, 141.33, 141.00, 139.91, 134.34, 128.88, 127.61, 127.31, 125.42, 125.17, 123.05, 120.90, 118.29, 111.07, 108.36. HRMS (MALDI-TOF), m/z: Calcd for C₅₅H₃₆N₂, 724.9070; Found, 725.6942. Anal. Calcd(%) for C₅₅H₃₆N₂: C, 91.13; H, 5.07; N, 3.86. Found: C, 91.13; H, 4.83; N, 3.82.

27-PTPhCNCZ:



In a 100 mL round flask, a mixture of 27-2BrCzCN (0.46 g, 1 mmol), PTBPin (1.04 g, 2.4 mmol), K_2CO_3 (5.52 g, 40 mmol), distilled water (20 mL), toluene (40 mL) and $Pd(PPh_3)_4$ (0.03 g, 0.03 mmol) was added and refluxed at 90 °C under N_2 atmosphere for 24 hours. The reaction was then quenched by water and the mixture was extracted with dichloromethane for three times. After evaporation of the solvent, the residue was purified via column chromatography and got white solid. (Yield: 84%). 1H NMR (500 MHz, CD_2Cl_2) δ (ppm): 8.31 (d, J = 8.1 Hz, 2H), 8.04 (d, J = 8.4 Hz, 2H), 7.92 (t, J = 2.8 Hz, 4H), 7.91 (d, J = 5.7 Hz, 3H), 7.88 (d, J = 6.4 Hz, 4H), 7.86 (s, 3H), 7.85 (s, 2H), 7.79 (d, J = 7.9 Hz, 9H), 7.75 (d, J = 1.2 Hz, 1H), 7.74 (d, J = 1.3 Hz, 2H), 7.55 (t, J = 7.7 Hz, 8H), 7.46 (t, J = 7.4 Hz, 4H). ^{13}C NMR (151 MHz, CD_2Cl_2) δ 142.40, 141.68, 141.34, 141.01, 140.66, 139.97, 139.23, 134.25, 128.89, 127.82, 127.72 – 127.36, 127.29, 125.20, 124.86, 123.01, 120.91, 120.52, 118.32, 110.95, 107.95. HRMS (MALDI-TOF), m/z: Calcd for $C_{67}H_{44}N_2$, 877.1030; Found, 878.0871. Anal. Calcd(%) for $C_{67}H_{44}N_2$: C, 91.75; H, 5.06; N, 3.19. Found: C, 91.19; H, 5.21; N, 3.01.

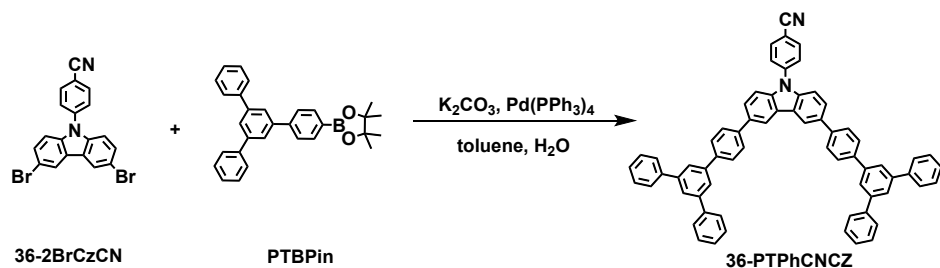
36-TPhCNCZ:



In a 100 mL round flask, a mixture of 36-2BrCzCN (0.46 g, 1 mmol), TPhB (0.66 g, 2.4 mmol), K_2CO_3 (5.52 g, 40 mmol), distilled water (20 mL), toluene (40 mL) and $Pd(PPh_3)_4$ (0.03 g, 0.03 mmol) was added and refluxed at 90 °C under N_2 atmosphere for 24 hours. The reaction was then quenched by water and the mixture was extracted with dichloromethane for three times. After evaporation of the solvent, the residue was purified via column chromatography and got white solid. (Yield: 76%). 1H NMR (500 MHz, CD_2Cl_2) δ (ppm): 8.64 (d, J = 1.1 Hz, 2H), 8.04 (s, 1H), 8.02 (d, J = 1.1 Hz, 4H), 7.94 (d, J = 1.3 Hz, 1H), 7.92 (d, J = 1.4 Hz, 1H), 7.91 (s, 1H), 7.89 (s, 1H), 7.88 (s, 2H), 7.83 (d, J = 5.9 Hz, 8H), 7.68 (d, J = 6.8 Hz, 3H), 7.56 (t, J = 6.1 Hz, 8H), 7.46 (t, J = 5.9 Hz, 4H). ^{13}C NMR (151 MHz, CD_2Cl_2) δ 142.45, 141.72, 141.15, 140.11, 134.19, 128.88, 127.82 – 127.46, 127.33, 126.96, 126.10, 125.10, 124.67, 119.21, 118.36, 110.69, 110.22. HRMS (MALDI-TOF), m/z: Calcd for $C_{55}H_{36}N_2$, 724.9070;

Found, 725.5176. Anal. Calcd(%) for $C_{55}H_{36}N_2$: C, 91.13; H, 5.07; N, 3.86. Found: C, 91.02; H, 5.03; N, 3.78.

36-PTPhCNCZ:



In a 100 mL round flask, a mixture of 36-2BrCzCN (0.46 g, 1 mmol), PTBPin (1.04 g, 2.4 mmol), K_2CO_3 (5.52 g, 40 mmol), distilled water (20 mL), toluene (40 mL) and $Pd(PPh_3)_4$ (0.03 g, 0.03 mmol) was added and refluxed at 90 °C under N_2 atmosphere for 24 hours. The reaction was then quenched by water and the mixture was extracted with dichloromethane for three times. After evaporation of the solvent, the residue was purified via column chromatography and got white solid. (Yield: 82%). 1H NMR (500 MHz, CD_2Cl_2) δ (ppm): 8.60 (s, 2H), 8.04 (d, J = 6.8 Hz, 3H), 7.95 (d, J = 3.7 Hz, 9H), 7.89 (t, J = 7.3 Hz, 6H), 7.81 (d, J = 6.3 Hz, 8H), 7.67 (d, J = 6.8 Hz, 4H), 7.56 (t, J = 6.1 Hz, 7H), 7.47 (t, J = 5.9 Hz, 5H). ^{13}C NMR (151 MHz, CD_2Cl_2) δ 142.63, 141.99, 141.30, 140.85, 140.27, 139.68, 134.33, 134.06, 129.13, 128.20 – 127.69, 127.55, 127.19, 126.10, 125.13, 119.10, 118.60, 115.13 – 114.82, 110.90, 110.47. HRMS (MALDI-TOF), m/z: Calcd for $C_{67}H_{44}N_2$, 877.1030; Found, 877.7209. Anal. Calcd(%) for $C_{67}H_{44}N_2$: C, 91.75; H, 5.06; N, 3.19. Found: C, 91.78; H, 4.97; N, 3.10.

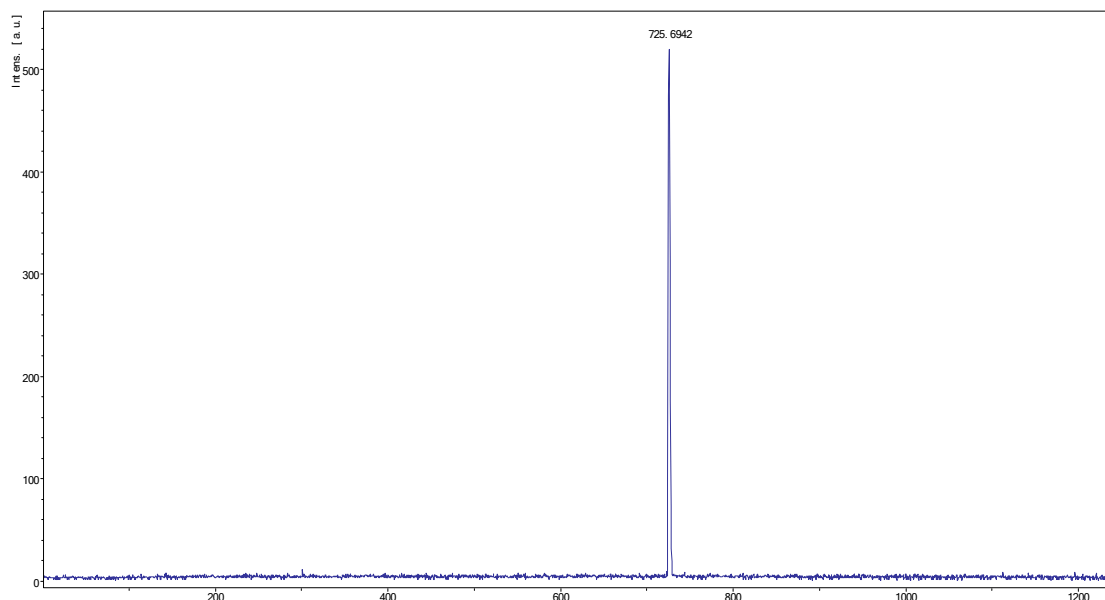


Fig. S1 HRMS spectrum of 27-TPhCNCZ.

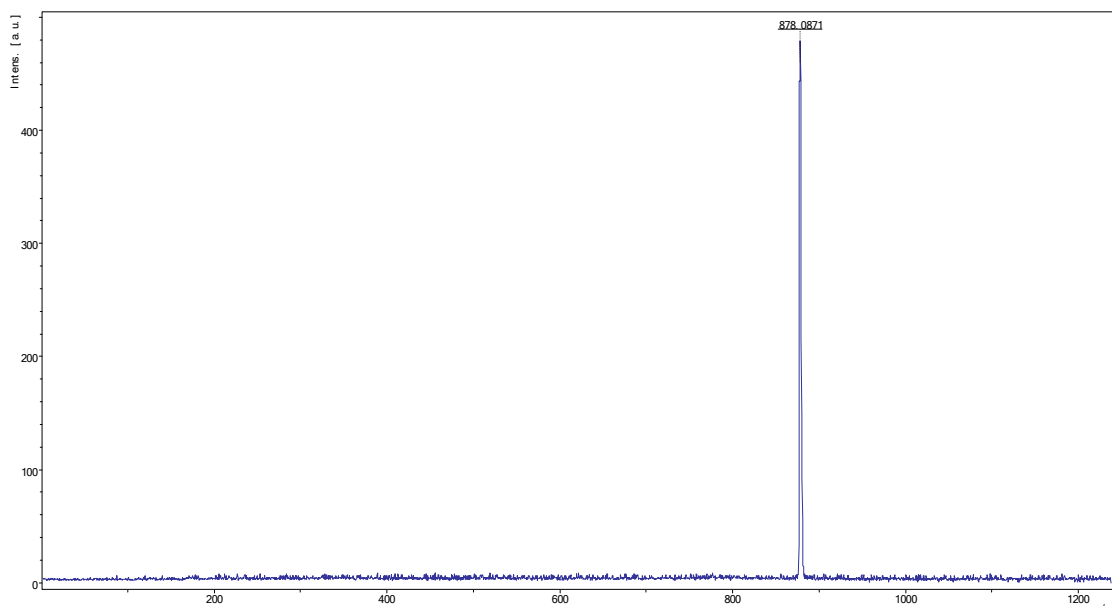


Fig. S2 HRMS spectrum of 27-PTPhCNCZ.

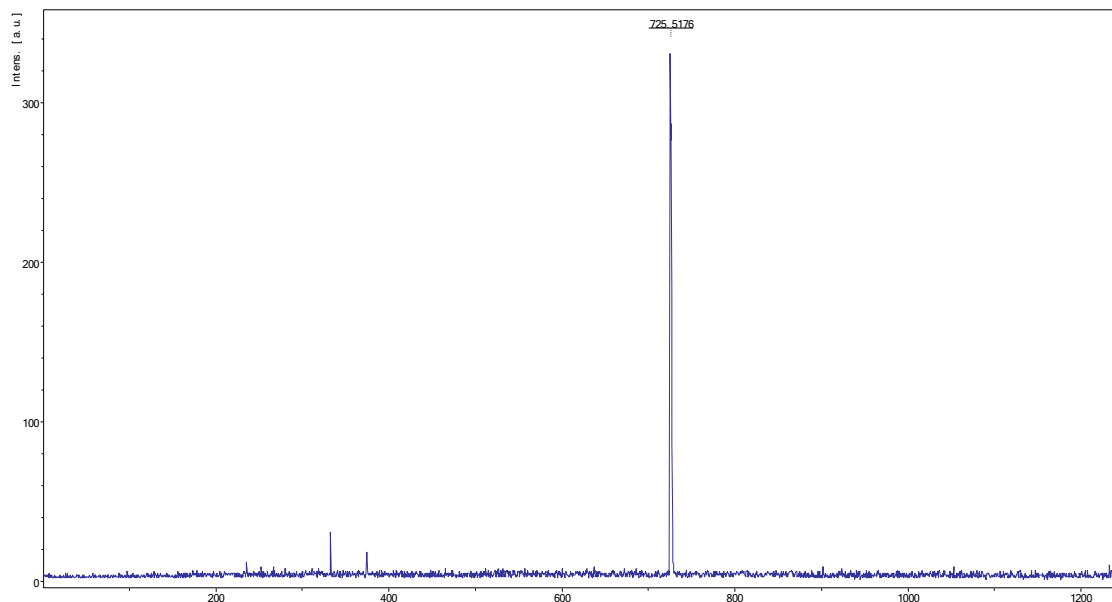


Fig. S3 HRMS spectrum of 36-TPhCNCZ.

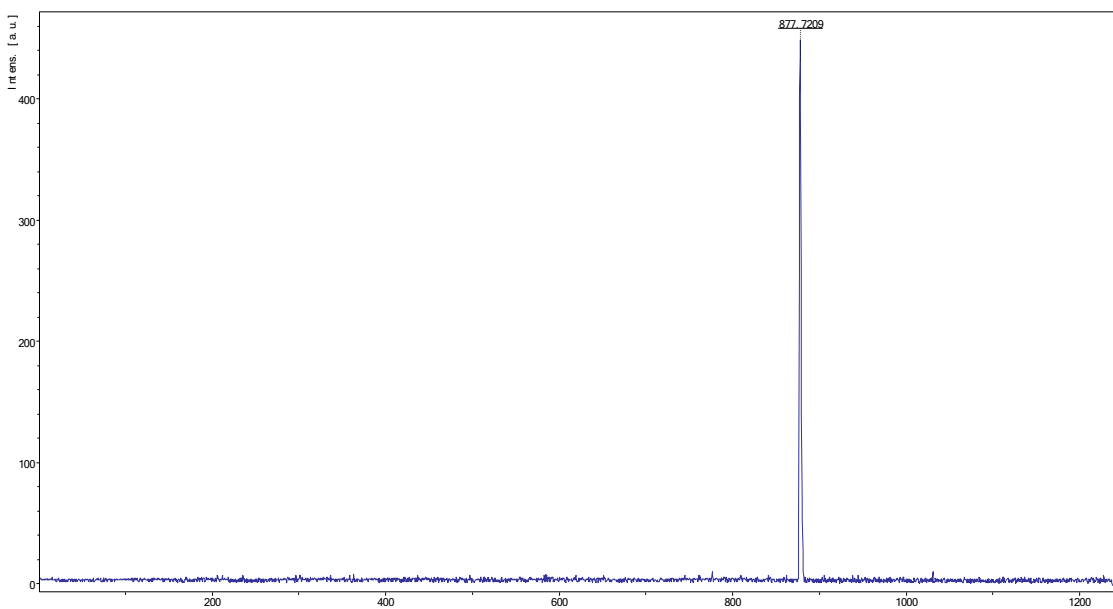


Fig. S4 HRMS spectrum of 36-PTPhCNCZ.

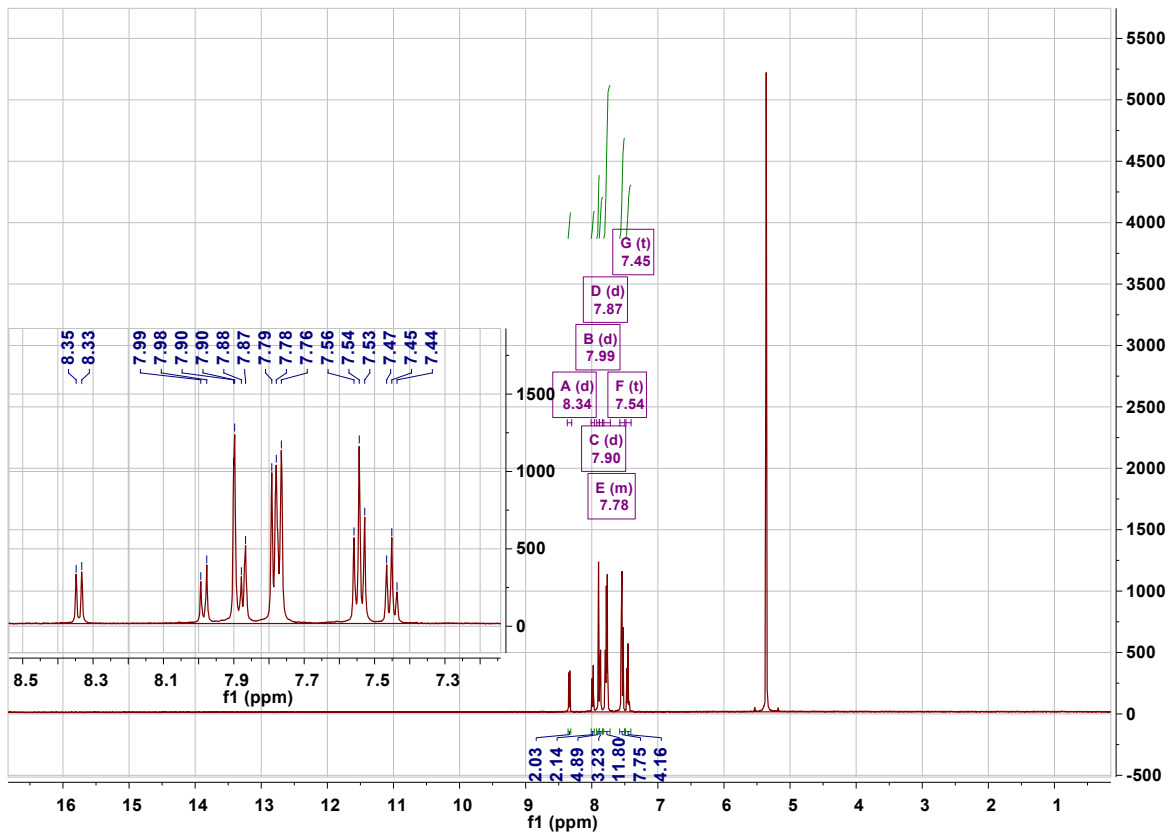


Fig. S5 ^1H NMR of 27-TPhCNCZ measured in CD_2Cl_2 .

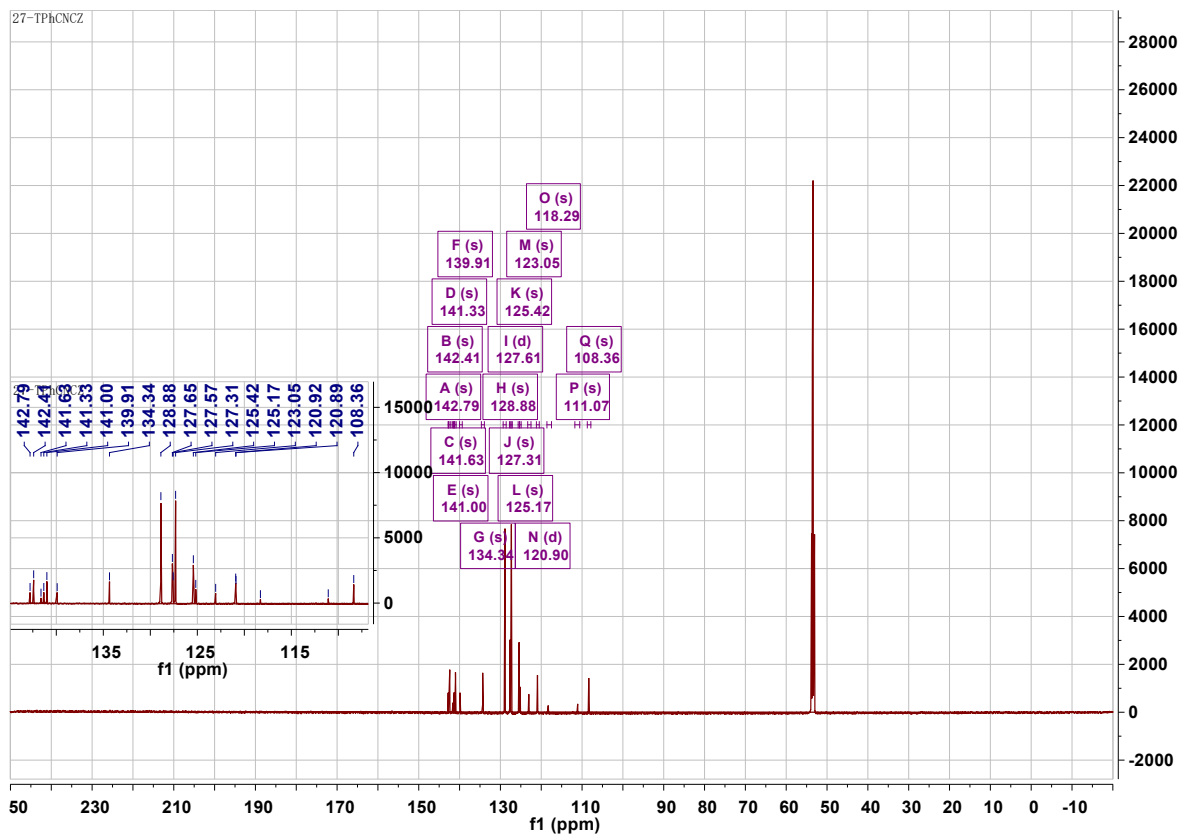


Fig. S6 ^{13}C NMR of 27-TPhCNCZ measured in CD_2Cl_2 .

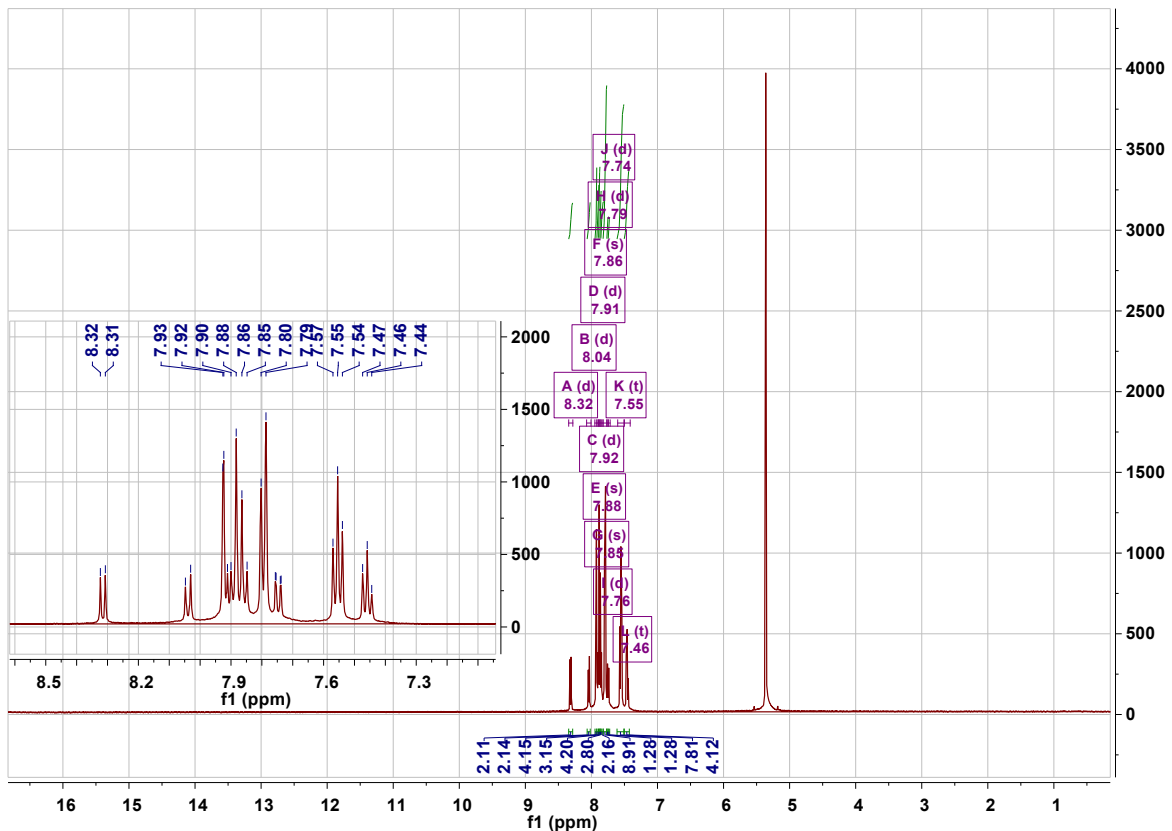


Fig. S7 ^1H NMR of 27-PTPhCNCZ measured in CD_2Cl_2 .

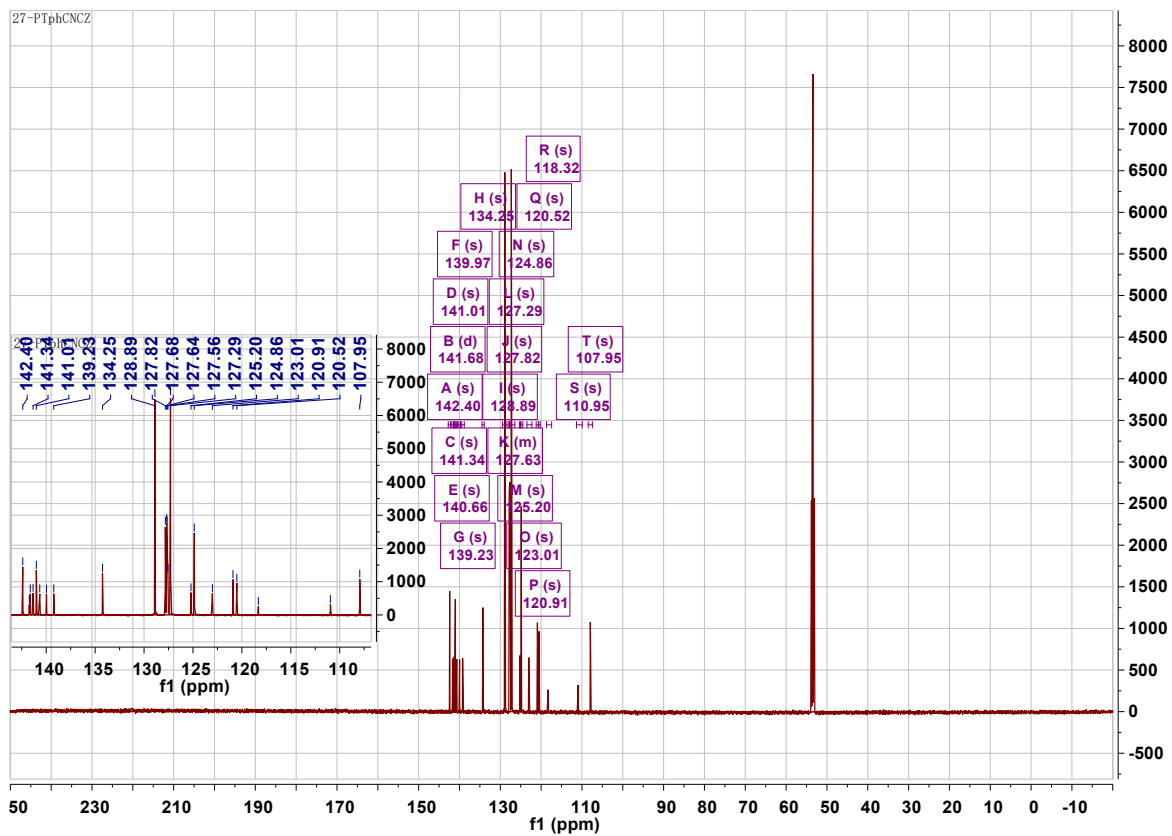


Fig. S8 ^{13}C NMR of 27-PTPhCNCZ measured in CD_2Cl_2 .

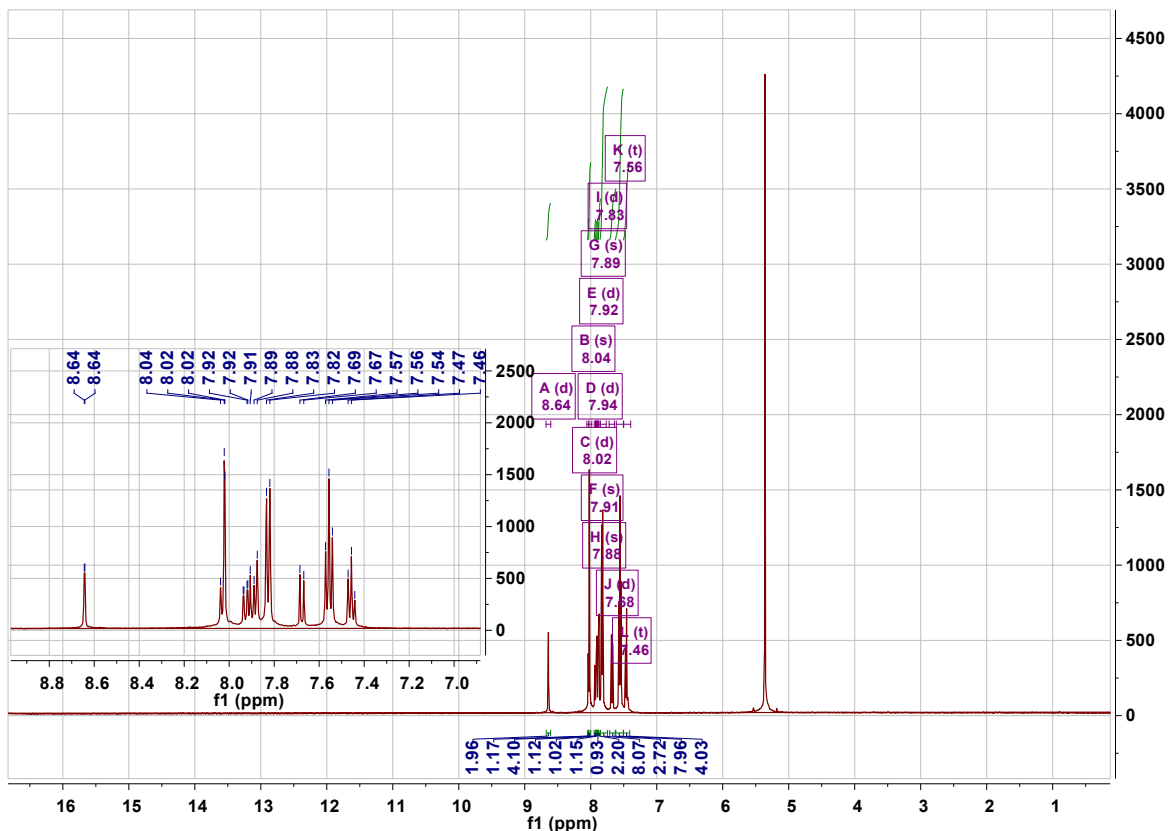


Fig. S9 ^1H NMR of 36-TPhCNCZ measured in CD_2Cl_2 .

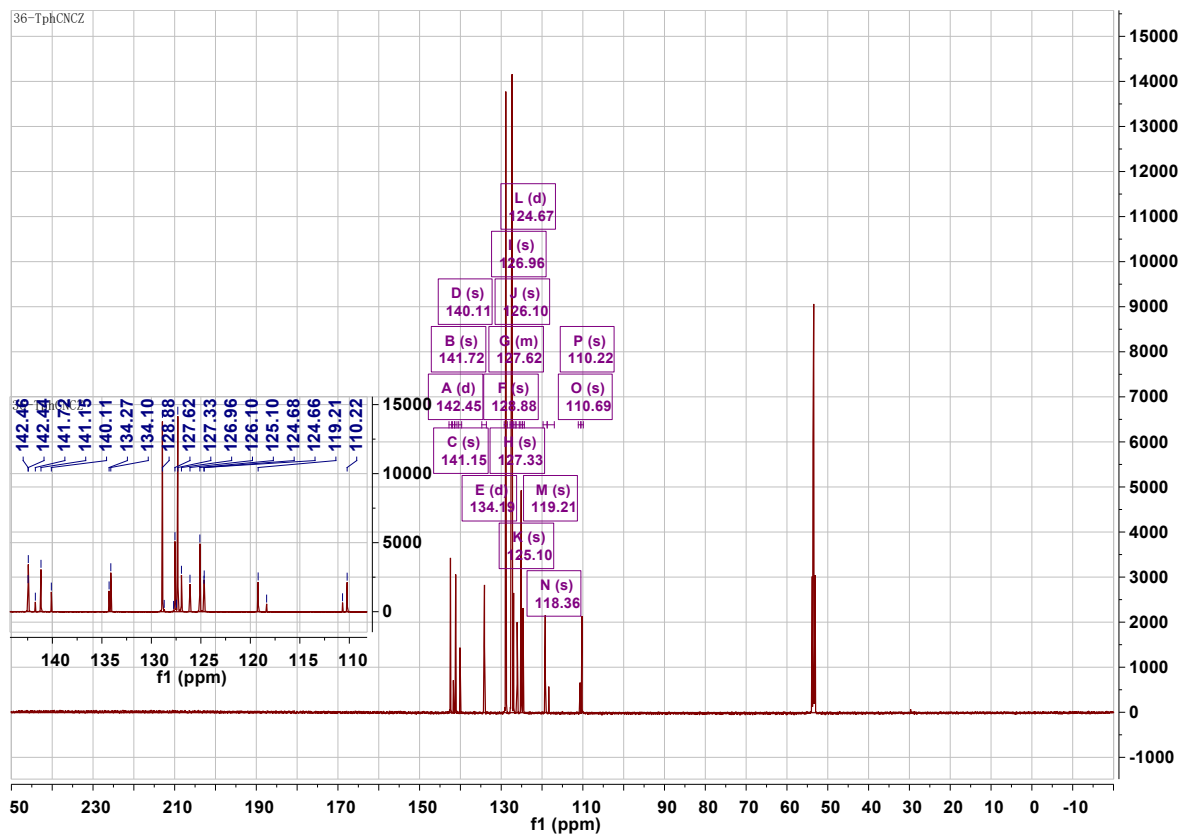


Fig. S10 ^{13}C NMR of 36-TPhCNCZ measured in CD_2Cl_2 .

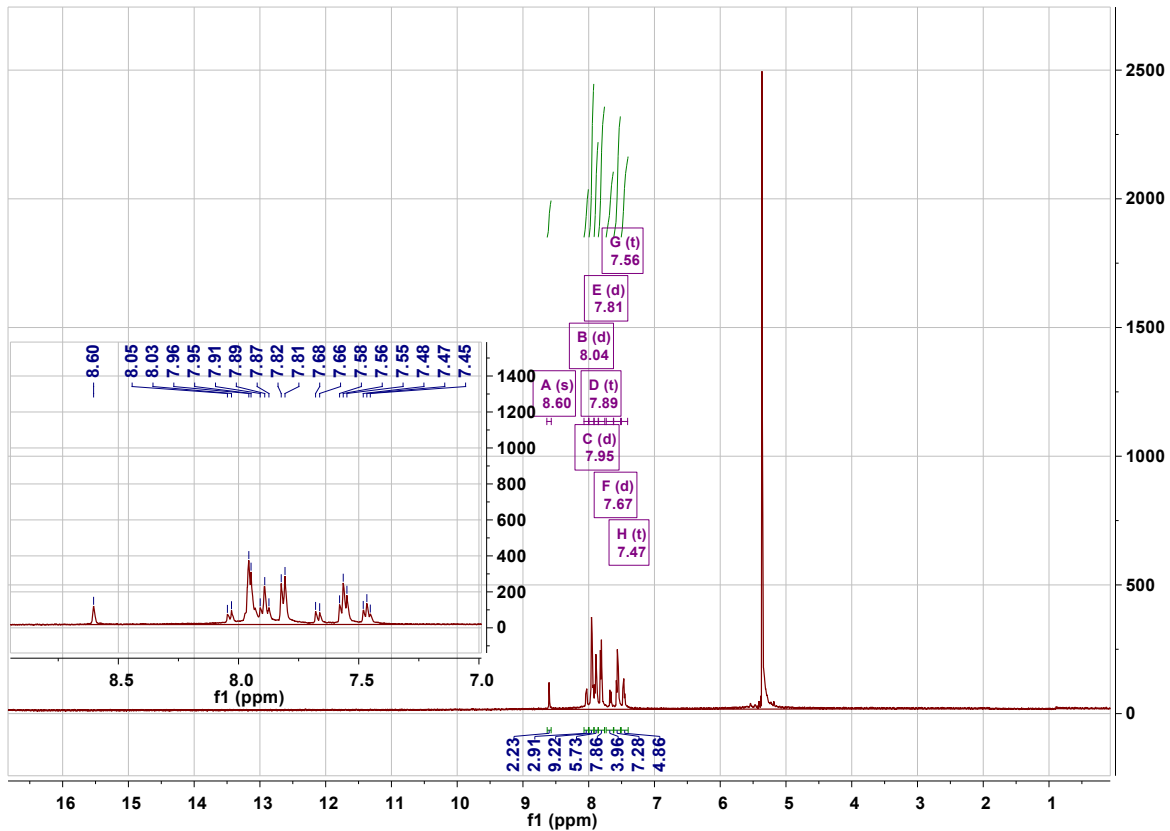


Fig. S11 ^1H NMR of 36-PTPhCNCZ measured in CD_2Cl_2 .

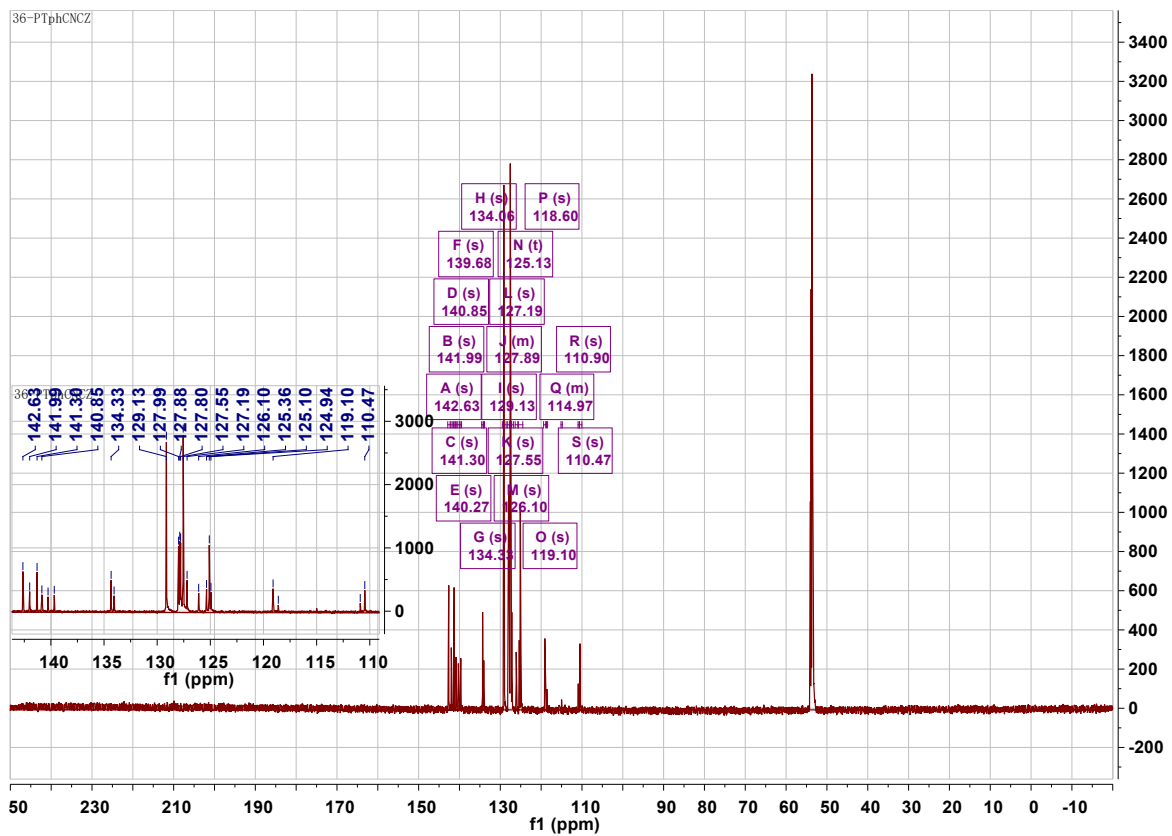


Fig. S12 ^{13}C NMR of 36-PTPhCNCZ measured in CD_2Cl_2 .

3. Thermal Properties

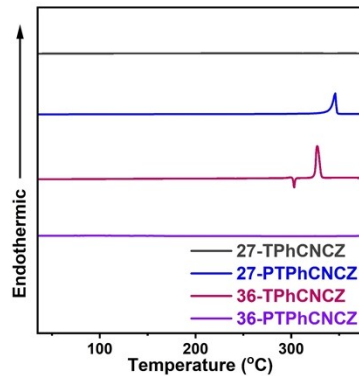


Fig. S13 DSC curves of 27-TPhCNCZ, 27-PTPhCNCZ, 36-TPhCNCZ, and 36-PTPhCNCZ.

4. Theoretical Calculations

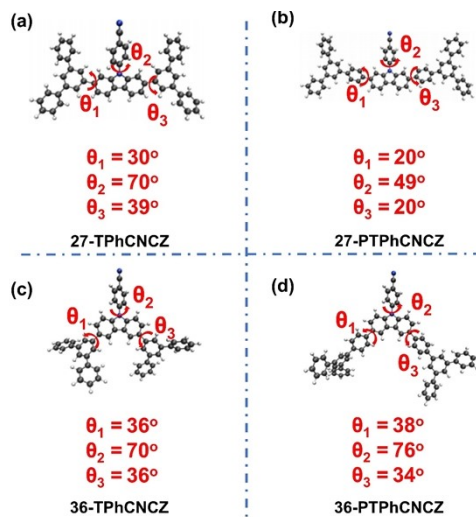


Fig. S14 Optimized geometries of 27-TPhCNCZ, 27-PTPhCNCZ, 36-TPhCNCZ and 36-PTPhCNCZ was performed at the PBE0/6-31G(d,p) level.

Table S1 Dihedral angles of 27-TPhCNCZ, 27-PTPhCNCZ, 36-TPhCNCZ and 36-PTPhCNCZ was performed at the PBE0/6-31G(d,p) level.

Compound	θ_1	θ_2	θ_3
27-TPhCNCZ	30°	70°	39°
27-PTPhCNCZ	20°	49°	20°
36-TPhCNCZ	36°	70°	36°
36-PTPhCNCZ	38°	76°	34°

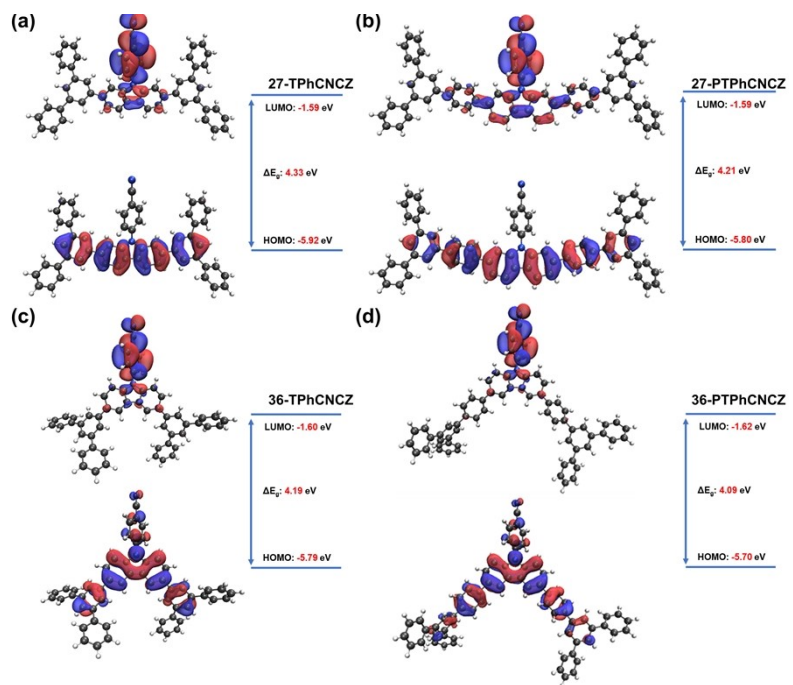


Fig. S15 The HOMO and LUMO of (a) 27-TPhCNCZ, (b) 27-PTPhCNCZ, (c) 36-TPhCNCZ, and (d) 36-PTPhCNCZ.

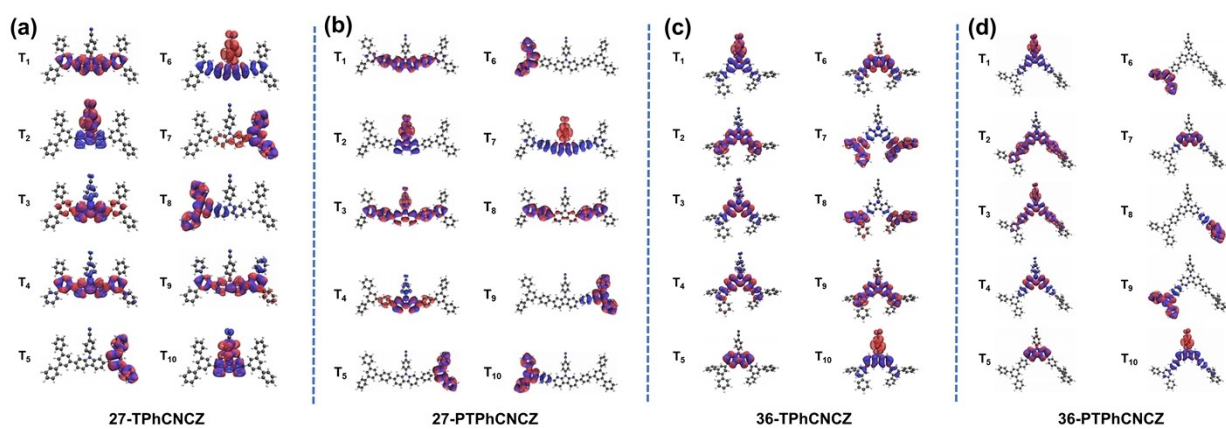


Fig. S16 The Analysis of NTOs of T_1 to T_{10} of (a) 27-TPhCNCZ, (b) 27-PTPhCNCZ, (c) 36-TPhCNCZ, and (d) 36-PTPhCNCZ, unoccupied (hole) (blue) & occupied (electron) (red).

5. Cyclic Voltammetry Measurement

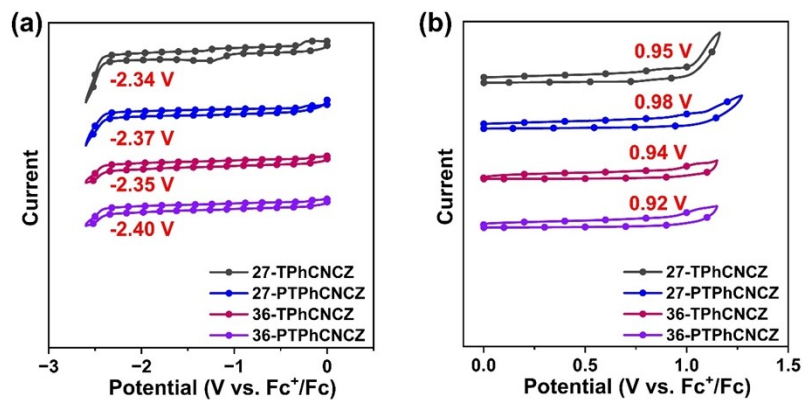


Fig. S17 Cyclic voltammogram of 27-TPhCNCZ, 27-PTPhCNCZ, 36-TPhCNCZ, and 36-PTPhCNCZ in (a) DMF (reduction) and (b) DCM (oxidation), measured with 0.1 M (Bu_4N) PF_6 as supporting electrolyte at a scan rate of 100 mV s⁻¹.

6. Photophysical Properties

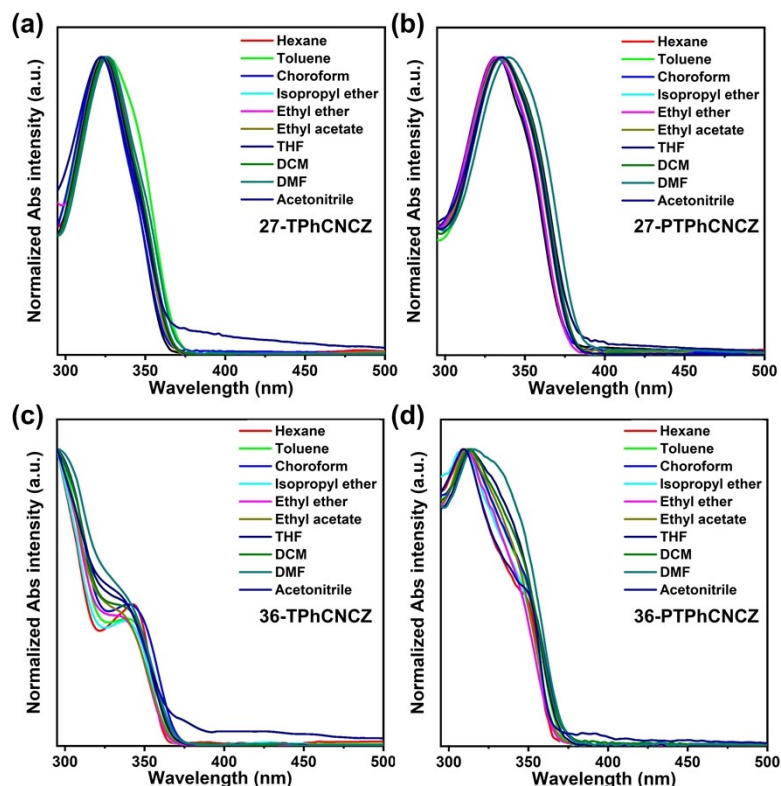


Fig. S18 Absorption spectra of (a) 27-TPhCNCZ, (b) 27-PTPhCNCZ, (c) 36-TPhCNCZ, and (d) 36-PTPhCNCZ in different polar solvents.

Table S2. The PLQYs of 27-PTPhCNCZ in various solvents in the solvatochromic measurement.

PLQY (%)	27-PTPhCNCZ
Hexane	72
Toluene	63
Chloroform	64
Isopropyl ether	57
Ethyl ether	53
Ethyl acetate	54
Tetrahydrofuran	50
Dichloromethane	54
Dimethylformamide	56
Acetonitrile	69

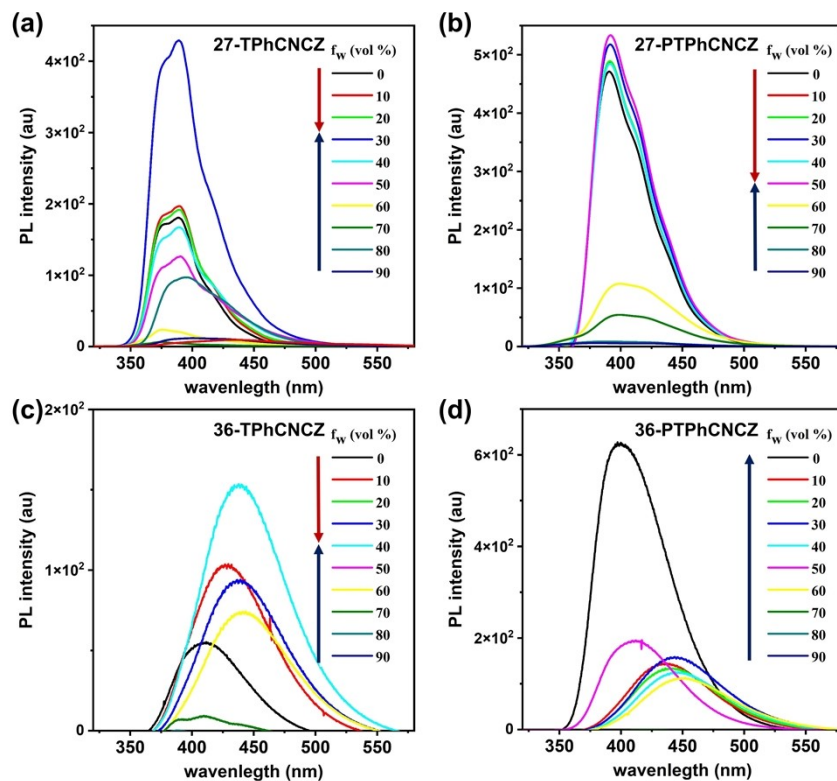


Fig. S19 PL spectra in mixture with different f_w for (a) 27-TPhCNCZ, (b) 27-PTPhCNCZ, (c) 36-TPhCNCZ, and (d) 36-PTPhCNCZ (10 mM).

7. Electroluminescence

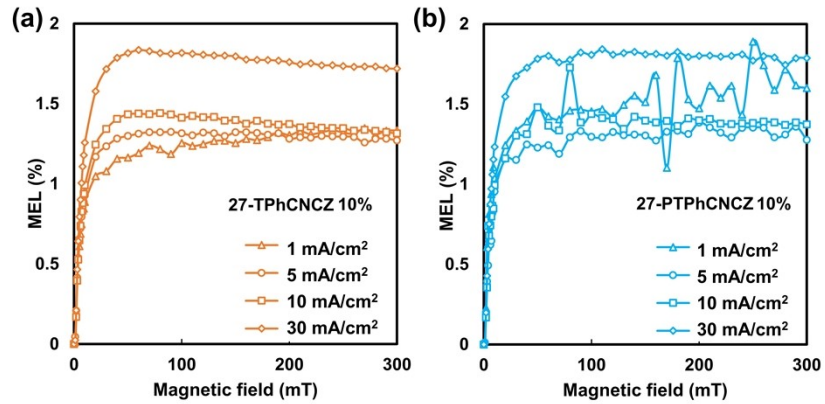


Fig. S20 Magneto-electroluminescence (MEL) response of (a) 27-TPhCNCZ and (b) 27-PTPhCNCZ 10 wt% doped OLED at 300 K.

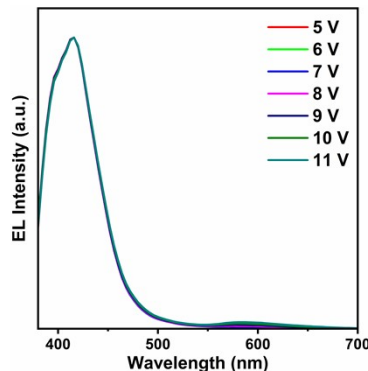


Fig. S21 The EL of doped OLED based on 27-PTPhCNCZ at different voltages.

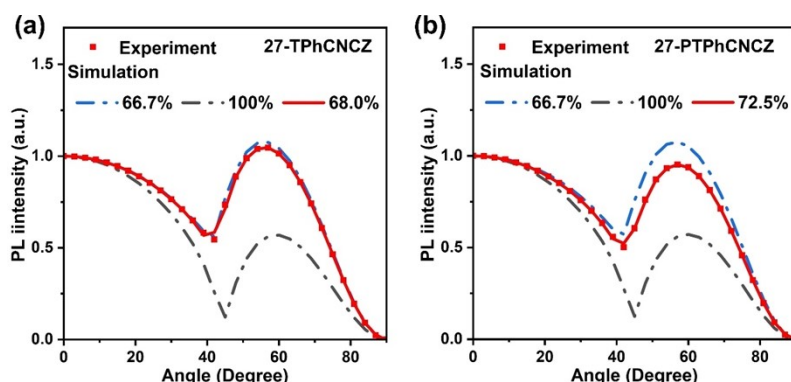


Fig. S22 The horizontal transition dipole orientation ratio ($\Theta//$) of 27-TPhCNCZ and 27-PTPhCNCZ in 10 wt% doped films.

References

1. B. Ma, B. Zhang, H. Zhang, Y. Huang, L. Liu, B. Wang, D. Yang, D. Ma, B. Z. Tang and Z. Wang, *Adv. Sci.*, 2024, **11**, 2407254.